Geosci. Model Dev. Discuss., 8, 3593–3651, 2015
www.geosci-model-dev-discuss.net/8/3593/2015/
doi:10.5194/gmdd-8-3593-2015

Geoscientific Model Development Discussions
Open Access

Simulating Secondary Inorganic Aerosols using the chemistry transport model MOCAGE version R2.15.0

J. Guth, B. Josse, V. Marécal, and M. Joly

Centre National de Recherches Météorologiques/Groupe d'étude de l'Atmosphère Météorologique, CNRS–Météo-France, UMR3589, Toulouse, France

Received: 30 March 2015 – Accepted: 8 April 2015 – Published: 29 April 2015

Correspondence to: J. Guth (jonathan.guth@meteo.fr)

Published by Copernicus Publications on behalf of the European Geosciences Union.

Abstract

In this study we develop a Secondary Inorganic Aerosol (SIA) module for the chemistry transport model MOCAGE developed at CNRM. Based on the thermodynamic equilibrium module ISORROPIA II, the new version of the model is evaluated both at the global scale and at the regional scale.

The results show high concentrations of secondary inorganic aerosols in the most polluted regions being Europe, Asia and the eastern part of North America. Asia shows higher sulfate concentrations than other regions thanks to emissions reduction in Europe and North America.

Using two simulations, one with and the other without secondary inorganic aerosol formation, the model global outputs are compared to previous studies, to MODIS AOD retrievals, and also to in situ measurements from the HTAP database. The model shows a better agreement in all geographical regions with MODIS AOD retrievals when introducing SIA. It also provides a good statistical agreement with in situ measurements of secondary inorganic aerosol composition: sulfate, nitrate and ammonium. In addition, the simulation with SIA gives generally a better agreement for secondary inorganic aerosols precursors (nitric acid, sulfur dioxide, ammonia) in particular with a reduction of the Modified Normalised Mean Bias (MNMB).

At the regional scale, over Europe, the model simulation with SIA are compared to the in situ measurements from the EMEP database and shows a good agreement with secondary inorganic aerosol composition. The results at the regional scale are consistent with those obtained with the global simulations. The AIRBASE database was used to compare the model to regulated air quality pollutants being particulate matter, ozone and nitrogen dioxide concentrations. The introduction of the SIA in MOCAGE provides a reduction of the $PM_{2.5}$ MNMB of 0.44 on a yearly basis and even 0.52 on a three spring months period (March, April, May) when SIA are maximum.

GMDD
8, 3593–3651, 2015

1 Introduction

Aerosols are a suspension of airborne solid or liquid particles, with a typical size between a few nanometres and 10 µm, that reside in the atmosphere for at least several hours (Stocker et al., 2013). Atmospheric aerosols play a key role in various fields. Their radiative properties allow them to absorb and scatter radiation and play a significant role into the global climate system especially in a climate change context. The estimation of radiative forcing due to aerosols is negative, but with a strong uncertainty. Most of aerosols seems to have a cooling effect except for black carbon (Stocker et al., 2013). This radiative aspect also affect the horizontal dimension while being a possible source of visibility reduction (Bäumer et al., 2008).

Aerosols are also important pollutants affecting air quality. Air quality is dealing with aerosols through the notion of particulate matter (PM). PM_x is the amount of particulate matter with diameters less than x microns. PM_{10} and $PM_{2.5}$ are used for the legal concentrations in air quality regulations. World Health Organization's guidelines for particulate matter are $20\,\mu g\,m^{-3}$ annual mean for PM_{10} and $10\,\mu g\,m^{-3}$ annual mean for $PM_{2.5}$ (WHO, 2006).

One can distinguish primary aerosols, directly emitted from sources, desert dust for example, and secondary aerosols, formed in the atmosphere from chemical and physical processes involving gaseous precursors. Secondary aerosols can be split into two types: Secondary Organic Aerosols (SOA) and Secondary Inorganic Aerosols (SIA). Gaseous precursors for SOA are Volatile Organic Compounds (VOCs), like isoprene for example, and correspond to a mixture of many different organic gases mainly composed of carbon, hydrogen and oxygen. Secondary inorganic aerosols main precursors are the gaseous species: ammonia, nitric acid and sulfuric acid. The proportion of SIA in the Particulate Matter is generally important. For example, in Europe, SIA represent between 30 and 50 % by mass of the $PM_{2.5}$ (Querol et al., 2004). Ammonia comes from emissions, while nitric acid and sulfuric acid mostly result from the oxidation of nitric oxides and sulfur dioxide, respectively. SIA are then controlled by the emissions of am-

GMDD
8, 3593–3651, 2015

monia, nitric oxides and sulfur dioxide, but also by the ambient conditions, temperature and humidity. While typical sources of nitric oxides are various (fossil fuel combustion, soils, biomass burning and lightning), sulfur compounds are mostly from anthropogenic sources and volcanoes. Ammonia emissions mostly come from domestic animals, excreta synthetic fertilizers, biomass burning and crops (Olivier et al., 1998).

Gas phase aerosol interactions result in modifications of the gas phase equilibrium. For example, the halogen chemistry over the marine boundary layer, especially chlorine chemistry, plays a role in ozone destruction and the oxidation of dimethyl sulfide (DMS). Chlorine is released from sea salts by acid displacement or photochemical processes (Saiz-Lopez and von Glasow, 2012).

Modelling the aerosols is important at the local scale but also at the regional and global scales. At the local or regional scales, modelling the aerosols is a way to provide air quality forecasts for PM_{10} and $PM_{2.5}$. At the global scale, aerosols modelling is important for taking properly into account the import and export of pollutants in the different regions of the world. It can also be used to study the evolution of the large scale background concentrations in current evolving climate conditions.

MOCAGE is the Chemical Transport Model (CTM) developed and used at CNRM/Météo-France. It is a global model including capability for simulating smaller domains with finer resolutions. MOCAGE is used for simulating stratospheric and tropospheric chemical concentrations (ozone for example) and also for air quality forecasts including ozone, nitrous oxides and aerosols. Recently, the model has been upgraded in order to account for the formation of secondary inorganic aerosols. These new developments are meant to be incorporated *in fine* into operational systems. The aim of this study is to evaluate the secondary inorganic aerosols in MOCAGE both at the global and regional (European) scales.

Section 2 presents the model MOCAGE including the newly developed secondary inorganic aerosol module. Then in Sect. 3 we define the experimental setup of the simulations and the observations used for the model evaluation. Results are discussed

GMDD
8, 3593–3651, 2015

in Sect. 4 for global simulations and Sect. 5 for regional simulations. Finally Sect. 6 concludes this study.

2 Model description

MOCAGE (*Modele de Chimie Atmospherique à Grande Echelle*) is an off-line global Chemistry Transport Model (CTM) used for research at Météo-France and serving in a wide range of scientific studies on tropospheric and stratospheric chemistry at various spatial and temporal scales. It was used for example for studying the impact of climate on chemistry (Teyssèdre et al., 2007; Lacressonnière et al., 2012; Lamarque et al., 2013) or tropospheric–stratospheric exchanges using data assimilation (El Amraoui et al., 2010; Barré et al., 2013). MOCAGE is also used for daily operational air quality forecasts in the framework of the French platform Prev'Air (Rouil et al., 2009, http://www2.prevair.org/) and in the European MACC-III (Monitoring Atmospheric Composition and Climate) project by being one of the seven models contributing to the ensemble forecasting system over the Europe (Marécal et al., 2015, http://macc-raq-op.meteo.fr/index.php).

2.1 Model geometry and inputs

MOCAGE can be used both as a global model and as a regional model. Thanks to its two-way grid-nesting capacity, it can use several overlapping grids. The typical resolution at the global scale is 2° longitude × 2° latitude, 0.5° longitude × 0.5° latitude at a regional scale and 0.1° longitude × 0.1° latitude at the local scale. MOCAGE has 47 levels from the surface up to 5 hPa. It uses a σ-pressure vertical coordinate giving a non-uniform resolution of about 40 m in the lower troposphere increasing to 800 m in the upper troposphere. There are seven levels in the planetary boundary layer, twenty in the free troposphere and twenty in the stratosphere.

GMDD
8, 3593–3651, 2015

MOCAGE, being an off-line CTM, gets its forcing fields from an independent meteorological driver. Meteorological fields driving MOCAGE are available every 3 or 6 h, and are linearly interpolated on one hour intervals, one hour being the dynamical time step of the model. Wind, temperature, humidity and pressure come from the IFS model (Integrated Forecast System) operated at ECMWF (European Centre for Medium-Range Weather Forecasts, http://www.ecmwf.int/) or from the ARPEGE model (*Action de Recherche Petite Echelle Grande Echelle*) operated at Météo-France (Courtier et al., 1991).

The chemical time-step used in the solver varies with altitude from 15 min in the stratosphere to a few seconds in the planetary boundary layer. Emissions are injected every 15 min, into the five lowest levels using an hyperbolic decay. Chemical fields are then updated every 15 min.

2.2 Gaseous species

2.2.1 Current chemistry scheme

MOCAGE uses two chemical schemes in order to represent both the tropospheric and the stratospheric air composition. The Regional Atmospheric Chemistry Mechanism (RACM) (Stockwell et al., 1997) is used in the troposphere while the REPROBUS scheme is used for the stratosphere (REactive Processes Ruling the Ozone BUdget in the Stratosphere) (Lefèvre et al., 1994).

The sulfur cycle has been completed compared to the initial RACM scheme. Following Boucher et al. (2002) and Pham et al. (1995), MOCAGE takes into account the aqueous oxidation reaction of sulfur dioxide into sulfuric acid (Ménégoz et al., 2009; Lacressonnière, 2012).

MOCAGE represents 111 gaseous compounds, 377 thermal reactions and 55 photolysis. Reaction rates are calculated during the simulation, every 15 min. The photolysis rates are interpolated every 15 min from a lookup table and modulated by account-

GMDD
8, 3593–3651, 2015

ing at each given point and time for the ozone column, solar zenith angle, cloud cover and surface albedo.

2.2.2 New developments for gaseous species

Ammonia (NH_3) has been added to the model species in order to account for the formation of the ammonium aerosols. No extra gaseous reaction involving ammonia has been added since they are slow enough to be neglected (Adams et al., 1999).

Dentener and Crutzen (1993) showed the reaction of hydrolysis of N_2O_5 on aerosols surface plays an important role in the atmosphere by lowering NO_x and O_3 concentrations. It has been added following Dentener and Crutzen (1993), with a reaction probability of 0.1.

2.3 Aerosols

2.3.1 Current aerosol module

The model in its current state is able to represent primary aerosols (Martet et al., 2009; Sič et al., 2015). The latest version of the primary aerosol scheme in MOCAGE has been evaluated by Sič et al. (2015). Sič et al. (2015) checked aerosols physical parameterization and proposed improvements. Based on simulations including only primary aerosols, they checked the consistency and validates the dry and wet deposition, the sedimentation and the emission processes.

MOCAGE uses the sectional approach with six size bins per type of aerosols, especially chosen to fit the different characteristics of each aerosol. Primary aerosols in MOCAGE are composed of four species: desert dust, sea salts, primary organic carbon and black carbon. Desert dust emissions are dynamically managed using Marticorena and Bergametti (1995) and divided into the bins using 3 modes of mean number diameters $r_1 = 0.64\,\mu m$, $r_2 = 3.45\,\mu m$ and $r_3 = 8.67\,\mu m$ of standard deviation $\sigma_1 = 1.7$,

GMDD
8, 3593–3651, 2015

σ_2 = 1.6 and σ_3 = 1.5. Desert dust emission is available over Sahara and Easter Asian desert.

Sea salts are dynamically managed following Gong (2003) with a sea surface temperature dependence (Jaeglé et al., 2011). The emission spectra is integrated over each bin range in order to use the information contained in the parameterization. Emissions of desert dusts and sea salts are calculated using the meteorological forcing at the resolution of each domain. Primary organic carbon and black carbon emissions are managed through emission inventories.

2.3.2 New developments of the aerosol module

In Sič et al. (2015), each type of aerosols uses specific size bins. Here we assume aerosols internal mixing. Therefore we use the same bin sizes for all types of aerosols, ranging from 2 nm to 50 µm with size bins limits: 2, 10, 100 nm, 1, 2.5, 10 and 50 µm. These new bin limits have been tested on a one year global simulation only with primary aerosols and compared to a simulation similar but with the aerosol specific size bins following Sič et al. (2015). The use of these new size bins gives similar results as using the aerosol dependent ones with a difference of less than 5 % on the forecast of PM_{10} and $PM_{2.5}$ burden on a annual mean on the global scale.

From this basis, it was possible to introduce secondary inorganic aerosols in MOCAGE. SIA results from a partition between the gaseous phase and the aerosols. This partition depends on compounds concentrations both into the gaseous and the aerosol phases and the ambient conditions: temperature and humidity. This partition can be solved using a thermodynamic equilibrium model. We choose for this purpose to use the latest version of the thermodynamic equilibrium model called ISORROPIA II (Nenes et al., 1998; Fountoukis and Nenes, 2007). ISORROPIA is commonly used in state-of-the-art CTMs for instance in CHIMERE (Bessagnet et al., 2004) and LOTOS-EUROS (Schaap et al., 2008). Sulfate, nitrate and ammonium aerosol concentrations are simulated by ISORROPIA, each of these species being represented in MOCAGE with six variable representing size bins. ISORROPIA gives the thermodynamic equi-

GMDD
8, 3593–3651, 2015

librium between 12 liquid aerosol species (see Table 1), 9 solid aerosol species (see Table 2) and 3 gaseous compounds (see Table 3). Wexler and Seinfeld (1990) showed that the time constant to achieve the equilibrium ranges from a few seconds for high aerosol mass concentrations and small aerosol sizes to more than a day for low mass concentrations and large particle radii. Nevertheless, we assume in MOCAGE that the equilibrium is reached in the 15 min chemical update frequency for the following reasons. The aim of the model is to be used mainly for air quality, especially the forecast of PM_{10} and $PM_{2.5}$. According to Capaldo et al. (2000), the forecast of total PM_{10} and $PM_{2.5}$ using an equilibrium method is in good agreement with more complex methods including a dynamic method. Moreover, for the operational use of MOCAGE, it is important to have the lowest computational cost possible. The equilibrium approach is about 400 times faster than a dynamic method and about 12 times faster than a hybrid approach (Capaldo et al., 2000).

ISORROPIA outputs are the total concentrations of different solid, liquid or gaseous compounds (see Tables 1–3). The aerosols outputs from ISORROPIA have then to be distributed over the MOCAGE model size bins. The secondary inorganic aerosols are distributed in the bins as follows. We assume that the compounds related to sea salts, meaning including sodium or chlorine, are distributed with the same size distribution as the sea salts aerosol variables in the model. Sea salts are emitted with a specific size distribution. Their time evolution in the model modifies this distribution because of the different physical phenomena affecting sea salts such as sedimentation (incorporating hygroscopicity) or wet and dry deposition. Thus at a given point at a given time, sea salts have a specific size distribution taking into account their evolution since the emission. ISORROPIA outputs including sodium or chlorine are distributed proportionally to this specific distribution.

The other compounds are distributed following the measured accumulation mode for SIA from Zhuang et al. (1999) (see Table 4). The fine mode is not used because of the lack of the coagulation processes in the model allowing mass transfer from the condensation mode to the accumulation mode. Thus by distributing only into the ac-

GMDD
8, 3593–3651, 2015

cumulation mode, we implicitly assume that the coagulation has already been acting to transform fine mode aerosols into accumulation mode aerosols. The coarse mode is also not used because the formation of coarse particle through reaction with sea salts is treated separately (cf. explanations in the previous paragraph). The remaining coarse particles, are assumed negligible. Indeed, Zhuang et al. (1999) found that sulfate coarse mode is mainly due to reaction of sulfur dioxide on sea salts or soil particles and nitrate coarse mode is mainly due to reaction of gas phase HNO_3 with sea salts particles. The nitrate and sulfate part reacting with sea salts is treated separately using the sea salt size distribution. They also found that ammonia gas prefers to react in fine mode. It forms coarse mode ammonium only if ammonia gas is present in excess to form ammonium chloride. This process is treated separately to form coarse mode ammonium through sea salts.

For example, we can consider two forms of nitrate $NaNO_3$ and $(NH_4)_2SO_4$. $NaNO_3$ results from an interaction between nitric acid (HNO_3) and sea salts (NaCl), this is why nitrate is split into size bins with the same proportions as the sea salts. $(NH_4)_2SO_4$ results from nitric acid (HNO_3) and sulfuric acid (H_2SO_4), then we will use measured modes from Zhuang et al. (1999) to distribute nitrate into the size bins.

2.4 Transport and physical parameterizations

MOCAGE uses a semi-lagrangian advection scheme (Williamson and Rasch, 1989) to transport chemical species at the resolved scale. For the convective transport, the numerical model uses the parameterization of Bechtold et al. (2001). The species are diffused by the turbulent mixing in the planetary boundary layer as described by the scheme of Louis (1979).

Dry deposition of gaseous compounds is taken into account following Wesely (1989). Wet deposition of gaseous species for the convective part is based on Mari et al. (2000) while the stratiform part from Liu et al. (2001) based on Giorgi and Chameides (1986).

Dry deposition of aerosols and gravitational settling are implemented as described in Seinfeld and Pandis (1998). The settling velocity is based on Stokes' law and is

GMDD
8, 3593–3651, 2015

a function of the particle diameter. Aerosol wet deposition takes into account in-cloud scavenging (Giorgi and Chameides, 1986), below-cloud scavenging (Slinn, 1977) and below-cloud scavenging due to snowfall (Slinn, 1982). For more details on sedimentation and wet deposition of aerosols, see Sič et al. (2015).

3 Experimental setup and observations

3.1 Simulations

Two series of simulations are conducted in order to evaluate the model secondary inorganic aerosol developments on the global and the regional scales. Two simulations were run at the global scale, at a resolution of 2° lon × 2° lat, for the year 2005. We chose the year 2005 because a large set of observations is available all over the world for this year. One of the simulations takes into account the newly integrated secondary inorganic aerosols (hereafter referred to as RACMSIA). The other one corresponds to the original version of MOCAGE without SIA (hereafter referred to as RACM). Simulations are run with a spin-up of 3 months and are driven by the meteorological fields from ARPEGE analyses.

The second series of simulations corresponds to a more recent period and focuses on the European domain to do an evaluation at the regional scale. Two simulations, with and without secondary inorganic aerosols, are conducted for the year 2010 and are compared to the EMEP measurement dataset. Both simulations have the global domain at 2° lon × 2° lat, and a nested European domain at 0.5° lon × 0.5° lat resolution. The latter domain covers the western part of the European continent between 16° W to 36° E and 32 to 72° N. The two domains communicate with each other by a two-way grid nesting scheme.

GMDD
8, 3593–3651, 2015

3.1.1 Gaseous and aerosols emissions

At the global scale, emissions used are the IPCC/AR5, representative for year 2000, for the anthropogenic species and biomass burning emissions (Lamarque et al., 2010). Biogenic emissions, representative for 1990, are based on GEIA. Nitrous oxides from lightning are taken into account following Price et al. (1997).

At the regional scale, over the European continent, the MACC project emissions, representative for the year 2009, are used for anthropogenic gaseous compounds (Kuenen et al., 2014) and completed by GEIA emissions for biogenic sources.

For aerosols, at the global scale, organic carbon and black carbon emissions used are those of the ACCMIP Project (Lamarque et al., 2010), while on a regional scale the MACC project emissions are used (Kuenen et al., 2014).

3.2 Observations for global simulation evaluation

MODIS daily mean AOD were used to evaluate to the model simulations. For this purpose, we use the daily MODIS data level 3 (L3, collection 5.1) for the year 2005 and perform an additional quality control and screening as presented in Sič et al. (2015). This processing is done to minimize the number of observations that are cloud contaminated and those with statistically low confidence which often artificially increase AOD (Zhang et al., 2005; Koren et al., 2007; Remer et al., 2008). Moreover, Ruiz-Arias et al. (2013) showed there is a rapid increase of the relative underestimation when the MODIS' L3 AODs are below 0.1. We then perform an additional screening by rejecting all AOD values below 0.05. Below this value, underestimation of AOD leads to a mean relative error higher than 50 % (Ruiz-Arias et al., 2013).

Aerosol Optical Depth (AOD) in MOCAGE are calculated at 550 nm using Mie theory with refractive indices taken from Global Aerosol Data Set (Köpke et al., 1997) and extinction efficiencies derived with Wiscombe's Mie scattering code for homogeneous spherical particles (Wiscombe, 1980).

GMDD
8, 3593–3651, 2015

For the model evaluation, we also use the HTAP observation database. It includes data from several measurement networks: EMEP, IMPROVE, NAtChem, EANET, CREATE, EUSAAR, NILU and the WMO-PCSAG global assessment precipitation dataset (http://www.htap.org/). Observations used are gaseous concentrations (nitric acid, nitric oxides, sulfur dioxide, ammonia), and the particulate matter composition (sulfate, nitrate, ammonium). The release used here is dated from 1 April 2014. Daily observations and weekly observations are used separately in order to consider comparisons at the same temporal scale. Daily observations cover both Europe countries and Canada. Weekly observations cover essentially the north of America and the eastern part of Asia. This is illustrated by Fig. 1 represents the location of the stations measuring sulfate aerosols. Note that the lack of ground observations in the Southern Hemisphere does not allow us to make the model evaluation in this part of the world, except for the comparison against MODIS AOD retrievals.

3.3 Observations for model evaluation over Europe

Evaluation at the regional scale is split into two parts. The first part is based on the EMEP observation database and is aimed to check the good simulation of secondary inorganic aerosols. Observation used are daily concentrations. The second part is based on the AIRBASE observation database. It is aimed to check the performance of the model against air quality monitoring stations observations on a hourly base.

3.3.1 EMEP database

The European Monitoring and Evaluation Programme (EMEP) is a scientifically based and policy driven programme under the Convention on Long-range Transboundary Air Pollution (CLRTAP) for international co-operation to solve transboundary air pollution problems (http://www.emep.int). Observations were downloaded through the EBAS repository (http://ebas.nilu.no). Daily observations are used to evaluate secondary inorganic aerosol composition (sulfate, nitrate, ammonium) over Europe. Figure 2 rep-

GMDD
8, 3593–3651, 2015

resents the location of the stations measuring nitrate aerosols on a daily basis. The EMEP monitoring sites are located such that significant local influence are minimised (Tørseth et al., 2012). Therefore measurements are assumed to be directly comparable to model outputs which are here at 0.5° × 0.5°.

3.3.2 AIRBASE database

To make a complementary evaluation, and because SIA directly affects major regulated air pollutants, we also make comparisons with air quality indicators monitored over Europe. For this we use AIRBASE, which is a dense measurement network used for air quality issues. It is managed by the European Topic Centre on Air Pollution and Climate Change Mitigation on behalf of the European Environment Agency. For this study, we use the latest version (version 8) of AIRBASE database (http://acm.eionet.europa.eu/databases/airbase). AIRBASE data are used in this study to evaluate the performance of the model on PM_{10}, $PM_{2.5}$, ozone and nitrogen dioxide forecast. For 2010, a total of 38 countries, including the 27 European Union countries have provided air quality data.

AIRBASE measuring stations are located on various sites: urban, periurban, rural, etc. In order to be able to compare model simulation at the 0.5° longitude × 0.5° latitude resolution, we select the stations which are representative of the model resolution. Following Joly and Peuch (2012), each station is characterised with a class between 1 and 10 according to its statistical characteristics, 1 corresponding to a fully rural behaviour and 10 to a highly polluted station. The selection of station is done following Lacressonnière et al. (2012) who conducted an evaluation of MOCAGE at the regional scale over several years. Only the stations corresponding to 1 to 5 classes are kept for ozone. For nitrogen dioxide, only the station corresponding to 1 and 2 classes are kept since nitrogen dioxide is a short lived species. For PM_{10} we select the stations with classes ranging from 1 to 5. Joly and Peuch (2012) do not provide a classification for $PM_{2.5}$. We choose to use for $PM_{2.5}$ the same stations as for PM_{10}.

GMDD
8, 3593–3651, 2015

3.4 Metrics used for evaluation

Several statistical indicators can be used for model evaluation against in situ data. In order to avoid misleading conclusions, Seigneur et al. (2000) recommended the use of the fractional bias and the fractional gross error instead of the bias and the root-mean-square error (rmse).

The fractional bias, also called modified normalized mean bias (MNMB) or mean fractional bias (MFB), used to quantify, for N observations, the mean between modeled (f) and observed (o) quantities is defined as follow:

$$\mathrm{MNMB} = \frac{2}{N}\sum_{i=1}^{N}\frac{f_i - o_i}{f_i + o_i} \tag{1}$$

The fractional bias ranges between −2 and 2 varying symmetrically with respect to under and overestimation.

The fractional gross error (FGE), also called mean fractional error (MFE) aims at quantifying the model error. It varies between 0 and 2 and is defined by:

$$\mathrm{FGE} = \frac{2}{N}\sum_{i=1}^{N}\left|\frac{f_i - o_i}{f_i + o_i}\right| \tag{2}$$

The correlation coefficient r indicates the extent to which patterns in the model match those in the observations and is defined by:

$$r = \frac{\frac{1}{N}\sum_{i=1}^{N}\left(f_i - \overline{f}\right)\left(o_i - \overline{o}\right)}{\sigma_f \sigma_o} \tag{3}$$

Where σ_f and σ_o are standard deviation respectively from the modelled and the observed time series and $\overline{f}$ and $\overline{o}$ their mean values.

GMDD
8, 3593–3651, 2015

Boylan and Russell (2006) give criteria to characterize a model performance against observations based on MNMB and FGE. It gives two types of performance. The "performance goal" is the level of accuracy that is considered to be close to the best a model can be expected to achieve. The "performance criteria" is the level of accuracy that is considered to be acceptable for modelling applications. For example, for particulate matter, for stations having a mean concentration superior to 2.25 $\mu g\,m^{-3}$ the "performance goal" is reached when the MNMB and the FGE are equal or less than ±0.3 and 0.5 respectively. These recommendations depend on the mean concentration of an observation point (see Table 1 in Boylan and Russell, 2006). In particular, low polluted stations might have large scores (MNMB and FGE) but still be satisfying.

4 Results and evaluation of the global simulations

This section presents results on the global scale. Firstly, we show and discuss the global concentrations before comparing results with measurements.

4.1 Global concentrations

Figure 3 represents the annual emission of the SIA precursors: sulfur dioxide, nitrous oxides and ammonia. Zones of highest emissions are mostly in the Northern Hemisphere located in the eastern part of Asia, North America and Europe. Ammonia emissions are more important in Europe and Eastern Asia than in North America. Ammonia and nitrous oxides also have high emissions in South America and Africa albeit to a lesser extent.

Figure 4 shows annual mean surface concentrations of the secondary inorganic compounds: sulfate, nitrate, ammonium and the sum of all these components. These fields are consistent with the emissions. High concentration zones correspond to zones of high emissions of precursors, being Europe, Eastern Asia and North America. However North America concentrations are slightly lower than the other areas of high con-

GMDD
8, 3593–3651, 2015

centrations. This might be due to the emissions of ammonia which are lower, being then less able to form aerosol with sulfate and nitrate. These mean annual secondary inorganic aerosol concentrations from MOCAGE are globally consistent in terms of geographical distribution and concentration values with Hauglustaine et al. (2014) model fields representative for 2000.

Figure 5 represents the comparison of HNO_3 and NH_3 annually mean concentrations between the RACM and the RACMSIA experiments. In the RACM experiment, ammonia does not chemically react. Dry and wet deposition are the only removal processes in this configuration. Ammonia is thus piling up with time in the model's atmosphere. In the RACMSIA experiment, ammonia is able to be used for aerosol production under favorable conditions (thermodynamic and availability of other inorganic compounds). Ammonia field in RACMSIA is more consistent then RACM with the modelling results from Xu and Penner (2012).

For HNO_3, the difference between the RACMSIA experiment and the RACM experiment is around 200 pptv less nitric acid for the RACMSIA experiment. In the RACM experiment, geographic patterns agree with Xu and Penner (2012), but concentrations are overestimated. In the RACMSIA experiment, part of nitric acid is transformed into aerosol and nitric acid concentrations are therefore lower and consistent with Xu and Penner (2012).

4.2 Comparison to MODIS AOD

Figure 6 presents the 2005 annual modified normalized mean bias against MODIS AOD observations. In Fig. 6, one can see that the Northern Hemisphere has a negative MNMB globally between −1 and −0.5 in the RACM experiment. In the RACMSIA experiment it is closer to 0 (between −0.5 and 0.5). This shows an improvement of the model AOD at the global scale when including SIA. This is confirmed by the global mean MNMB which is −0.41 for RACM experiment and −0.21 for RACMSIA experiment. Sič et al. (2015) made a similar comparison: AOD against MOCAGE simulations. They conclude their study by stating that one reason of MOCAGE negative bias in AOD

GMDD
8, 3593–3651, 2015

might be due to the lack of secondary aerosols in their model version. Here we show that adding secondary inorganic aerosols improve MOCAGE results. The global modified normalised mean bias remains negative, but this is expected since the secondary organic aerosols are still missing in the model.

When comparing Fig. 6 with Fig. 4 one can notice that areas where AODs are increased correspond to areas where secondary inorganic aerosol concentrations are the most important, i.e. in Europe, Asia and Eastern part of the North America. Near the coasts, where the influence from the land is stronger, the bias is negative in the RACM experiment and is closer to zero by taking into account secondary inorganic aerosols (RACMSIA). In the Guinea Golf, the improvement is noteworthy but the MNMB is still negative. This could be due to insufficient biomass-burning aerosol emissions, especially through secondary organic aerosols formation, or to too low desert dust aerosol emissions.

4.3 Atmospheric chemical composition against HTAP observations

In this section, we use the daily observations as one time series to calculate the statistics. This allows us to give the same weight to every observation instead of every measuring station because measuring stations do not always provide the full set of observations for the whole year.

Modelled fields are interpolated at the observation location. We take the field concentration at the surface, knowing that the altitude difference between the model and the actual station altitude can lead to significant differences. This is why stations with an altitude difference higher than 1000 m with the model orography have been suppressed for the statistics. After this screening, there are 98 stations left on daily observations (104 before screening). For weekly observations, there are 214 stations left (225 before screening).

GMDD
8, 3593–3651, 2015

4.3.1 Daily observations

Table 5 presents the statistical results against daily observations for the main components of the secondary inorganic aerosols: sulfate, nitrate and ammonium. As presented in Fig. 1 this type of observations is mainly located in Europe and Canada. Sulfate measurements are divided into two parts, sulfate total and sulfate corrected. The sulfate corrected corresponds to non sea salt sulfate (nss). The use of non sea salt sulfate is better for our comparison because we do not have sulfate emissions combined with sea salts. But to have the largest number of stations, we use both measures.

Sulfate total are underestimated, with a MNMB of −0.32 which is expected according the lack of sea salt sulfates. With a correlation of 0.52, the model performs fairly well. Sulfate corrected are better modelled with a correlation of 0.70. They are slightly underestimated with a MNMB of −0.12. Ammonium are slightly overestimated with a MNMB of 0.19, and with a good correlation of 0.69. Nitrate are also well modeled with a low MNMB of 0.13, a fairly good correlation (0.53) but with a relatively high FGE (0.94).

The model is able to well simulate the time-series at a given point. As an example, Fig. 7 shows the time-series of sulfate, nitrate and ammonium daily observations against MOCAGE values at an Irish measuring station. We choose this station because it is placed in a rural location. It is also not under direct urban activity and on the way of chemical export from North America. Nevertheless the concentrations at this station are not very low and have variations. The model performs well on the three components by capturing the daily variations and their values. Statistics over this station are given in Table 6. The calculated values in Table 6 are consistent with Fig. 7. MOCAGE is able to represent well the SIA components with low MNMB and FGE and good correlations.

We also checked the behaviour of the model against the diagnostic proposed by Boylan and Russell (2006). As expected, sulfate corrected, all of the 21 the stations are well modelled according to both criteria ("performance goal" and "performance criteria"). Sulfate total are not as well represented by the model, out of 94 stations, 9 do not comply with the "performance criteria" and 16 do not respect the "performance goal".

GMDD
8, 3593–3651, 2015

For nitrate, only 2 stations do not respect both diagnostics over a set of 61 stations. There are 51 stations measuring ammonium concentrations and only 6 stations do not fit the "performance goal" while all do for the "performance criteria". The Boylan and Russell (2006) perspective comfort the good performance of the model for secondary inorganic aerosols compounds.

Table 7 presents the statistics for gaseous precursors of SIA both for RACM and RACMSIA experiments. Sulfur dioxide is not really affected by the SIA because there are no direct reactions newly integrated in the model. Oxidation of sulfur dioxide into sulfate was already taken into account in the RACM simulation. But the scores for ammonia are significantly improved. The correlation rises from 0.18 to 0.33, the fractional gross error drops from 1.84 to 1.27 and the modified mean mean bias from 1.84 to 0.79. The nitrogen dioxide statistics are slightly better with the fractional gross error which decreases from 0.83 to 0.77 with SIA formation. Nitric acid seems better simulated with SIA formation looking at the MNMB, but the fractional gross error and the correlation are worse in the RACMSIA simulation including secondary inorganic aerosols. Depending on atmospheric conditions, SIA formation can be either a sink or a source of nitric acid. Also nitric acid undergoes many other processes that drive its concentration. Therefore simulating nitric acid variations with time and space is challenging and is not only related to the ability of the model to produce realistic SIA. This is why it is difficult to interpret nitric acid performances.

In summary on HTAP daily data, concerning Europe and Canada, the model is able to well simulate secondary inorganic aerosols. We note that the model tends to overestimate ammonium and ammonia. There is also an overestimation of sulfur dioxide while sulfates are slightly underestimated. Nevertheless these comparisons shows the ability of the model to reproduce secondary inorganic aerosols on a global scale. It also shows than on a specific location the model is able to reproduce very well the SIA concentrations and their temporal evolution.

GMDD
8, 3593–3651, 2015

4.3.2 Weekly observations

Table 8 presents the statistical results against weekly observations for the main components of secondary inorganic aerosols. As presented in Fig. 1, weekly observations are mainly located in North America and Asia, so this type of observations is complementary to the daily ones. For sulfate, one can see that sulfate total is slightly underestimated but well simulated with a correlation coefficient of 0.66. Sulfate corrected should not be interpreted as a general behaviour because there is only one measuring station in this case. As for daily observations, ammonium are overestimated with a MNMB of 0.34 and a FGE of 0.84. Similarly to daily observations, nitrates MNMB is low with a similar FGE of 1.00. As for the daily observations, the bias is low but the error is fairly high.

For gaseous compounds, statistics are not presented here because there are only between 16 and 28 stations depending on the parameter and there are no nitrogen dioxide measures. Nevertheless the behaviour on this limited number of stations is similar to that of the daily observations.

Figure 1 presents the location of the HTAP stations used in this study. By looking at the weekly station localisation, one can see that there are two main groups of stations, one in North America and one in Asia. By splitting the dataset between Asian and American stations, there are 29 stations for the Asian area and 156 for the American one. The results are presented in Table 9.

Sulfates, based on total sulfate data, has a MNMB similar in both zones, but the correlation is better in North America (0.67) than in Asia (0.38). Nitrates are better simulated in North America. Indeed, MNMBs are 0.30 and 0.05 in Asia and North America, respectively. Moreover, the correlation is also better (0.41) than in Asia (0.13). MNMB of ammonium is also worse in Asia (0.35) than in North America (0.27). Nevertheless, correlation of ammonium is better in Asia (0.41) against North America (0.19).

When comparing Figs. 1 and 6 one can observe that North American stations are located on areas where the model underestimates the AOD when simulating SIA while

GMDD
8, 3593–3651, 2015

the Asian stations are located on areas where the AODs are well simulated by the model when taking into account SIA. When looking at stations in North America, comparisons to in situ measurements shows a good agreement for SIA fields. The negative bias on Fig. 6 over this area might then be due to the lack of secondary organic aerosols in the model. The Asian stations comparisons however shows an overestimation of SIA. The good results on AOD comparison might there be due to an overestimation of SIA in this area and a compensation on AODs.

5 Results and evaluation of the regional simulation

The first set of simulations, showed the model was able to simulate correctly SIA on the global scale. The next step is to check the behaviour of the model on a regional domain, Europe, with a better resolution and different emission inventories.

This section presents results on the second set of simulation over the year 2010 including two nested domains: the global one (at 2° lon × 2° lat) and a regional one (at 0.5° lon × 0.5° lat). As we already looked at model results on a global scale (see Sect. 4), the focus in this section is put on the regional European domain. Firstly we analyse the results before comparing them with measurements from EMEP database for secondary inorganic aerosols components. Then we make a comparison to AIRBASE measurements from an air quality point of view.

5.1 European concentration fields

Figure 8 presents SIA precursor emissions (SO_2, NO_x and NH_3) for the year 2010 on the regional domain. SO_2 emissions are maximum in an area covering the Benelux, England and Central Europe. NO_x emissions are important almost everywhere in Western Europe but with a maximum emission in Benelux and England. NH_3 is emitted everywhere except in Scandinavia with maxima in Brittany (France), Benelux and Po Valley (Italy).

GMDD
8, 3593–3651, 2015

Figure 9 presents the annual mean surface concentration for year 2010 over the regional domain. SIA are present almost everywhere especially over the continent, with very high concentrations in the Po valley, Benelux and Central Europe.

Sulfate aerosols are mainly present in the Central Europe. This is due to the high emission zone of SO_2 in this region. These results are consistent with Schaap et al. (2004) who simulated the year 1995. Schaap et al. (2004) also found high sulfate concentrations over Benelux and England. There are no high sulfate concentrations over these locations in our simulation. These differences are due to the emission reduction program. Indeed Western Europe has strongly decreased its SO_2 emissions since 1995.

Nitrate aerosols are mainly present in Benelux and the Po Valley. Benelux has high nitrate concentrations due to high NO_x emissions in this area, while Po Valley has not such high NO_x emissions, but a climate and a topography which favour pollution events.

Ammonium aerosols is less important in terms of mass concentration and is more smoothly distributed over the domain. Ammonium is present where either sulfate or nitrate are present, because the main SIA components are ammonium sulfates and ammonium nitrates.

Figure 10 presents the comparison of HNO_3 and NH_3 annual mean concentration between the RACM and the RACMSIA experiments. Similarly to the global simulation, HNO_3 and NH_3 concentrations are lowered in the RACMSIA experiment compared to the RACM experiment. Compared to Schaap et al. (2004) NH_3 concentrations are too high in the RACM experiment while having closer values in the RACMSIA experiment. Patterns are also similar except for the Po Valley where MOCAGE simulates very high concentrations of ammonia. Concerning HNO_3, patterns are the same for both experiment, RACM and RACMSIA.

GMDD
8, 3593–3651, 2015

5.2 Atmospheric chemical composition over a regional domain against EMEP observations

For this part, the observations are used in the same way as for the global scale. However here we only use daily observations because there are very few weekly observations (between 3 and 5 stations depending on the parameter observed).

Table 10 presents the statistical results for the main components of the secondary inorganic aerosols: sulfate, nitrate and ammonium. Sulfate, total and corrected are both underestimated with an MNMB of −0.36 and −0.35 respectively and a FGE of 0.75 and 0.74. Correlation is slightly better (0.68) for sulfate corrected than for sulfate total (0.58). Ammonium are only slightly overestimated, with an MNMB of 0.18, and well modelled with a correlation of 0.71.

Table 11 presents the statistics for the gaseous precursors of SIA. The model has a similar behaviour as on the global scale against daily HTAP observations. In both simulations, the species with the best perfomances is NO_2 while the one with the worse scores is NH_3. The use of SIA mainly affects NH_3 with a very significant improvement of all statistical indicators. The differences between the model results and the observations can partly be explained by uncertainties in the emission inventories used. In (Kuenen et al., 2014), they report uncertainties in ammonia emission of about 50 %. For NO_x, uncertainties are lower but still about 30 %. SO_2 only has about 10 % uncertainty. These uncertainties in emission might explain differences for the couple of species ammonia and ammonium and for nitrogen dioxide. For sulfur compounds, there is an underestimation of sulfate aerosols and a strong overestimation of SO_2 which can not be explained only by the emission uncertainties. The oxidation process transforming SO_2 into sulfuric acid depends on several variables (gaseous concentrations, liquid water content, temperature, etc). It is therefore more difficult to represent correctly since all these variables have also some associated uncertainties.

GMDD
8, 3593–3651, 2015

5.3 Air quality indicators

In order to complete the validation, we check the change on air quality pollutants due to the introduction of secondary inorganic aerosols. These indicators are surface concentrations of O_3 and NO_x (NO and NO_2) for gaseous species and PM_{10} and $PM_{2.5}$ for aerosols.

We also examine the impact of the seasonal basis which is here based on three seasons statistics: spring (March, April and May), summer (June, July, August) and fall (September, October and November). Winter is not analyzed here because winter months (December, January and February) are not simulated as a continuous series.

5.3.1 Particulate matter forecast: $PM_{2.5}$ and PM_{10}

Table 12 presents statistics for $PM_{2.5}$ over Europe for the year 2010 based on AIRBASE hourly observations. One can see that $PM_{2.5}$ are better represented in the RACMSIA version. Indeed, MNMB increases from −0.58 in RACM to −0.14 in RACMSIA and the FGE decreasing from 0.77 in RACM to 0.56 in RACMSIA. MOCAGE still underestimates $PM_{2.5}$, but the error is smaller with the new version of the model MOCAGE with SIA. The correlation also rises from 0.47 to 0.58. Secondary organic aerosols are still missing in the model and likely explain the $PM_{2.5}$ negative bias. Table 12 also presents the statistics for PM_{10} over Europe for the year 2010 based on AIRBASE hourly observations. The conclusions are the same as for $PM_{2.5}$ but with bigger figures as for $PM_{2.5}$ statistics.

Table 13 presents the variation of $PM_{2.5}$ MNMB according to the season. The Δ represents the improvement of the RACMSIA experiment compared to the RACM experiment. Since the MNMB are all negative, a positive value of Δ means that adding secondary inorganic aerosols has a positive effect on the simulation.

Over the whole year, the MNMB is improved by 0.44. By looking at the behaviour on the different seasons, one can see than in spring (MAM) the improvement of $PM_{2.5}$ forecasts is larger than for the other seasons (0.52). When taking a look to the PM_{10}

GMDD
8, 3593–3651, 2015

seasonal variability, the conclusion is the same. This behaviour is due to the fact that spring, especially March and April, is the most favourable period for secondary inorganic aerosols formation in Europe. In Summer, the MNMB is improved by 0.35 in the RACMSIA simulation, which is very significant. But the normalised bias in RACMSIA experiment is higher than for the other seasons. This is due to the fact that summer is a season favourable to secondary organic aerosol, still lacking in our model, especially with a biogenic origin. Indeed, biogenic volatile organic compound as isoprene for example, have higher emissions in summer which leads to higher biogenic secondary organic aerosols in summer.

5.3.2 Feedback on the gaseous chemistry

Figure 11 represents the annual mean concentrations of surface ozone for the RACM and the RACMSIA experiments. One can see a significant decrease of surface ozone, especially over oceans, between 5 and 10 ppbv. On land, concentrations are nearly the same. By being absorbed into the aerosol phase, nitric acid is not available for forming NO_x again and then the ozone equilibrium is displaced. The effect is less important over the land because of the proximity of NO_x sources which drive the nitrous oxides concentrations.

Table 12 presents the statistics for ozone against hourly observations from the AIRBASE database. The statistics are very similar between the two experiments, only the MNMB is slightly better for the RACMSIA experiment. It is linked with the ozone maps showing a decrease over the ocean while the field is similar over land. Although the ozone maps show a decrease over the ocean the field is similar over land where the AIRBASE stations are located.

Table 12 presents the statistics for nitrogen dioxide against hourly observations from the AIRBASE database. All statistical indicators are close in both experiments (RACM and RACMSIA) indicating that the NO_2 equilibrium in MOCAGE is not affected by the introduction of SIA in the model. The comparison between Tables 11 and 12 shows that the MOCAGE simulations have similar performances against EMEP and AIRBASE. For

GMDD
8, 3593–3651, 2015

this statistics we use 44 EMEP stations and 610 AIRBASE stations. This shows that MOCAGE model with or without SIA provides robust NO_2 fields at the surface even when compared to a large number of data.

6 Conclusions

In this study we developed a secondary inorganic aerosol module into the CTM MOCAGE. We showed that the model is able to represent secondary inorganic aerosols on both the global scale and the European regional scale. The different constituents of the secondary inorganic aerosols being sulfate, nitrate and ammonium simulated by the model fit well against the different observational datasets used: HTAP and EMEP. These databases and the AIRBASE database were also used to assess gaseous species concentrations. Comparisons show a neutral impact of SIA on SO_2 and NO_2, a mixed impact on HNO_3 (with a much better MNMB but slightly worse FGE and correlation) and a large improvement of NH_3. Simulations with SIA does not show a significant improvement on statistical scores for ozone. Nevertheless, there is an impact on ozone fields at surface over sea that is important but very little change over land as reflected by the scores. The comparison with satellite AODs shows that the global aerosol budget is significantly better when SIA are used in the model. Finally, the model is able to perform generally very well at reproducing daily variations of SIA as illustrated by the comparison between MOCAGE and observations at a station in Ireland.

By comparing the MOCAGE model results to the AIRBASE dataset over Europe in terms of particulate matter concentration, we showed that the model performs also better with the introduction of secondary inorganic aerosols. Especially in spring (March, April, May), the MNMB of the $PM_{2.5}$ is improved 0.52 rising from −0.55 to −0.03. Over the full year of simulation, there is still a negative bias in $PM_{2.5}$ and PM_{10} concentrations, which can be due to the lack of secondary organic aerosols in the model. The

GMDD
8, 3593–3651, 2015

implementation of secondary organic aerosols in MOCAGE is the next major development foreseen to fully complete the aerosol scheme.

Model simulations with SIA show that SO_2 is significantly overestimated and the sulfates are underestimated. For instance at the regional scale, the SO_2 MNMB is 1.15 and the sulfates MNMB is −0.36. This indicates that the model is not able to fully convert SO_2 into sulfates. This can be related to several sources of uncertainty within the conversion process such as temperature, liquid water content and its pH, gaseous concentrations of precursors that are partly linked to their emissions (Kuenen et al., 2014). Some work will be done in the future to identify the main sources of uncertainties in order to improve the representation of the SO_2 oxidation process into sulfuric acid. Concerning ammonia and ammonium, they have both positive bias that can at least be partly explained by the large uncertainties in ammonia emissions of about 50 % (Kuenen et al., 2014).

In the implementation, we made choices for representing phenomena favouring computational efficiency over a very detailed representation while keeping a good accuracy. One of the final goals is to integrate this module for operational forecasts into the Prev'Air and the COPERNICUS programs. The model MOCAGE will also be used to make research studies including long run simulations for instance for the CCMI program (Chemistry–Climate Model initiative) and the analysis of the aerosol budget in the Mediterranean area.

Code availability

This paper is based on source code that is presently incorporated inside the MOCAGE model. The MOCAGE source code is the property of Météo-France and CERFACS, and it is based on libraries that belong to some other holders. The MOCAGE model is not open source and routines from MOCAGE cannot be freely distributed. Therefore, we cannot provide the code openly to the GMD website.

GMDD
8, 3593–3651, 2015

Acknowledgements. We would like to thank Athanasios Nenes for providing us the ISORROPIA II source code (http://www.isorropia.eas.gatech.edu/). This work has been possible thanks to the AIRBASE, EMEP and HTAP database. We also acknowledge the MODIS mission team and scientists for the production of the data used in this study

References

Adams, P. J., Seinfeld, J. H., and Koch, D. M.: Global concentrations of tropospheric sulfate, nitrate, and ammonium aerosol simulated in a general circulation model, J. Geophys. Res.-Atmos., 104, 13791–13823, 1999. 3599

Barré, J., Peuch, V.-H., Lahoz, W., Attié, J.-L., Josse, B., Piacentini, A., Eremenko, M., Dufour, G., Nedelec, P., von Clarmann, T., and El Amraoui, L.: Combined data assimilation of ozone tropospheric columns and stratospheric profiles in a high-resolution CTM, Q. J. Roy. Meteor. Soc., 140, 966–981, 2013. 3597

Bäumer, D., Vogel, B., Versick, S., Rinke, R., Möhler, O., and Schnaiter, M.: Relationship of visibility, aerosol optical thickness and aerosol size distribution in an ageing air mass over South-West Germany, Atmos. Environ., 42, 989–998, 2008. 3595

Bechtold, P., Bazile, E., Guichard, F., Mascart, P., and Richard, E.: A mass-flux convection scheme for regional and global models, Q. J. Roy. Meteor. Soc., 127, 869–886, 2001. 3602

Bessagnet, B., Hodzic, A., Vautard, R., Beekmann, M., Cheinet, S., Honoré, C., Liousse, C., and Rouil, L.: Aerosol modeling with CHIMERE – preliminary evaluation at the continental scale, Atmos. Environ., 38, 2803–2817, 2004. 3600

Boucher, O., Pham, M., and Venkataraman, C.: Simulation of the Atmospheric Sulfur Cycle in the Laboratoire de Météorologie Dynamique General Circulation Model: Model Description, Model Evaluation, and Global and European Budgets, Scientific note from the IPSL Institut Pierre-Simon Laplace 21, 2002. 3598

Boylan, J. W. and Russell, A. G.: {PM} and light extinction model performance metrics, goals, and criteria for three-dimensional air quality models, Atmos. Environ., 40, 4946–4959, doi:10.1016/j.atmosenv.2005.09.087, 2006. 3608, 3611, 3612

Capaldo, K. P., Pilinis, C., and Pandis, S. N.: A computationally efficient hybrid approach for dynamic gas/aerosol transfer in air quality models, Atmos. Environ., 34, 3617–3627, 2000. 3601

GMDD

8, 3593–3651, 2015

Courtier, P., Freydier, C., Geleyn, J., Rabier, F., and Rochas, M.: The ARPEGE Project at Météo-France, ECMWF workshop, European center for Medium-Range Weather Forecast, Reading, England, 1991. 3598

Dentener, F. J. and Crutzen, P. J.: Reaction of N_2O_5 on tropospheric aerosols: impact on the global distributions of NO_x, O_3, and OH, J. Geophys. Res.-Atmos., 98, 7149–7163, 1993. 3599

El Amraoui, L., Attié, J.-L., Semane, N., Claeyman, M., Peuch, V.-H., Warner, J., Ricaud, P., Cammas, J.-P., Piacentini, A., Josse, B., Cariolle, D., Massart, S., and Bencherif, H.: Midlatitude stratosphere – troposphere exchange as diagnosed by MLS O_3 and MOPITT CO assimilated fields, Atmos. Chem. Phys., 10, 2175–2194, doi:10.5194/acp-10-2175-2010, 2010. 3597

Fountoukis, C. and Nenes, A.: ISORROPIA II: a computationally efficient thermodynamic equilibrium model for K^+–Ca^{2+}–Mg^{2+}–NH_4^+–Na^+–SO_4^{2-}–NO_3^-–Cl^-–H_2O aerosols, Atmos. Chem. Phys., 7, 4639–4659, doi:10.5194/acp-7-4639-2007, 2007. 3600

Giorgi, F. and Chameides, W. L.: Rainout lifetimes of highly soluble aerosols and gases as inferred from simulations with a general circulation model, J. Geophys. Res.-Atmos., 91, 14367–14376, 1986. 3602, 3603

Gong, S.: A parameterization of sea-salt aerosol source function for sub-and super-micron particles, Global Biogeochem. Cy., 17, 1097, doi:10.1029/2003GB002079, 2003. 3600

Hauglustaine, D. A., Balkanski, Y., and Schulz, M.: A global model simulation of present and future nitrate aerosols and their direct radiative forcing of climate, Atmos. Chem. Phys., 14, 11031–11063, doi:10.5194/acp-14-11031-2014, 2014. 3609

Jaeglé, L., Quinn, P. K., Bates, T. S., Alexander, B., and Lin, J.-T.: Global distribution of sea salt aerosols: new constraints from in situ and remote sensing observations, Atmos. Chem. Phys., 11, 3137–3157, doi:10.5194/acp-11-3137-2011, 2011. 3600

Joly, M. and Peuch, V.-H.: Objective classification of air quality monitoring sites over Europe, Atmos. Environ., 47, 111–123, 2012. 3606

Köpke, P., Hess, M., Schult, I., and Shettle, E.: Global Aerosol Data Set, Max-Planck-Institut für Meteorologie, Hamburg, Germany, 1997. 3604

Koren, I., Remer, L. A., Kaufman, Y. J., Rudich, Y., and Martins, J. V.: On the twilight zone between clouds and aerosols, Geophys. Res. Lett., 34, L08805, doi:10.1029/2007GL029253, 2007. 3604

GMDD
8, 3593–3651, 2015

Kuenen, J. J. P., Visschedijk, A. J. H., Jozwicka, M., and Denier van der Gon, H. A. C.: TNO-MACC_II emission inventory; a multi-year (2003–2009) consistent high-resolution European emission inventory for air quality modelling, Atmos. Chem. Phys., 14, 10963–10976, doi:10.5194/acp-14-10963-2014, 2014. 3604, 3616, 3620

Lacressonnière, G.: Etude par modélisation numérique de la qualité de l'air en Europe dans les climats actuel et futur, PhD thesis, Université Toulouse III – Paul Sabatier, Centre National de Recherches Météorologiques/Groupe d'étude de l'Atmosphère Météorologique, CNRS-Météo-France, Toulouse, France, 2012. 3598

Lacressonnière, G., Peuch, V.-H., Arteta, J., Josse, B., Joly, M., Marécal, V., Saint Martin, D., Déqué, M., and Watson, L.: How realistic are air quality hindcasts driven by forcings from climate model simulations?, Geosci. Model Dev., 5, 1565–1587, doi:10.5194/gmd-5-1565-2012, 2012. 3597, 3606

Lamarque, J.-F., Bond, T. C., Eyring, V., Granier, C., Heil, A., Klimont, Z., Lee, D., Liousse, C., Mieville, A., Owen, B., Schultz, M. G., Shindell, D., Smith, S. J., Stehfest, E., Van Aardenne, J., Cooper, O. R., Kainuma, M., Mahowald, N., McConnell, J. R., Naik, V., Riahi, K., and van Vuuren, D. P.: Historical (1850–2000) gridded anthropogenic and biomass burning emissions of reactive gases and aerosols: methodology and application, Atmos. Chem. Phys., 10, 7017–7039, doi:10.5194/acp-10-7017-2010, 2010. 3604

Lamarque, J.-F., Shindell, D. T., Josse, B., Young, P. J., Cionni, I., Eyring, V., Bergmann, D., Cameron-Smith, P., Collins, W. J., Doherty, R., Dalsoren, S., Faluvegi, G., Folberth, G., Ghan, S. J., Horowitz, L. W., Lee, Y. H., MacKenzie, I. A., Nagashima, T., Naik, V., Plummer, D., Righi, M., Rumbold, S. T., Schulz, M., Skeie, R. B., Stevenson, D. S., Strode, S., Sudo, K., Szopa, S., Voulgarakis, A., and Zeng, G.: The Atmospheric Chemistry and Climate Model Intercomparison Project (ACCMIP): overview and description of models, simulations and climate diagnostics, Geosci. Model Dev., 6, 179–206, doi:10.5194/gmd-6-179-2013, 2013. 3597

Lefèvre, F., Brasseur, G., Folkins, I., Smith, A., and Simon, P.: Chemistry of the 1991–1992 stratospheric winter: three-dimensional model simulations, J. Geophys. Res.-Atmos., 99, 8183–8195, 1994. 3598

Liu, H., Jacob, D. J., Bey, I., and Yantosca, R. M.: Constraints from 210Pb and 7Be on wet deposition and transport in a global three-dimensional chemical tracer model driven by assimilated meteorological fields, J. Geophys. Res.-Atmos., 106, 12109–12128, 2001. 3602

GMDD
8, 3593–3651, 2015

Louis, J.-F.: A parametric model of vertical eddy fluxes in the atmosphere, Bound.-Lay. Meteorol., 17, 187–202, 1979. 3602

Marécal, V., Peuch, V.-H., Andersson, C., Andersson, S., Arteta, J., Beekmann, M., Benedictow, A., Bergström, R., Bessagnet, B., Cansado, A., Chéroux, F., Colette, A., Coman, A., Curier, R. L., Denier van der Gon, H. A. C., Drouin, A., Elbern, H., Emili, E., Engelen, R. J., Eskes, H. J., Foret, G., Friese, E., Gauss, M., Giannaros, C., Guth, J., Joly, M., Jaumouillé, E., Josse, B., Kadygrov, N., Kaiser, J. W., Krajsek, K., Kuenen, J., Kumar, U., Liora, N., Lopez, E., Malherbe, L., Martinez, I., Melas, D., Meleux, F., Menut, L., Moinat, P., Morales, T., Parmentier, J., Piacentini, A., Plu, M., Poupkou, A., Queguiner, S., Robertson, L., Rouïl, L., Schaap, M., Segers, A., Sofiev, M., Thomas, M., Timmermans, R., Valdebenito, Á., van Velthoven, P., van Versendaal, R., Vira, J., and Ung, A.: A regional air quality forecasting system over Europe: the MACC-II daily ensemble production, Geosci. Model Dev. Discuss., 8, 2739–2806, doi:10.5194/gmdd-8-2739-2015, 2015. 3597

Mari, C., Jacob, D. J., and Bechtold, P.: Transport and scavenging of soluble gases in a deep convective cloud, J. Geophys. Res.-Atmos., 105, 22255–22267, 2000. 3602

Martet, M., Peuch, V., Laurent, B., Marticorena, B., and Bergametti, G.: Evaluation of long-range transport and deposition of desert dust with the CTM MOCAGE, Tellus B, 61, 449–463, 2009. 3599

Marticorena, B. and Bergametti, G.: Modeling the atmospheric dust cycle: 1. Design of a soil-derived dust emission scheme, J. Geophys. Res.-Atmos., 100, 16415–16430, 1995. 3599

Ménégoz, M., Salas y Melia, D., Legrand, M., Teyssèdre, H., Michou, M., Peuch, V.-H., Martet, M., Josse, B., and Dombrowski-Etchevers, I.: Equilibrium of sinks and sources of sulphate over Europe: comparison between a six-year simulation and EMEP observations, Atmos. Chem. Phys., 9, 4505–4519, doi:10.5194/acp-9-4505-2009, 2009. 3598

Nenes, A., Pandis, S., and Pilinis, C.: ISORROPIA: a new thermodynamic equilibrium model for multiphase multicomponent inorganic aerosols, Aquat. Geochem., 4, 123–152, doi:10.1023/A:1009604003981, 1998. 3600

Olivier, J., Bouwman, A., Van der Hoek, K., and Berdowski, J.: Global air emission inventories for anthropogenic sources of NO_x, NH_3 and N_2O in 1990, Environ. Pollut., 102, 135–148, 1998. 3596

Pham, M., Müller, J.-F., Brasseur, G., Granier, C., and Megie, G.: A three-dimensional study of the tropospheric sulfur cycle, J. Geophys. Res., 100, 26061–26092, 1995. 3598

GMDD
8, 3593–3651, 2015

Price, C., Penner, J., and Prather, M.: NO_x from lightning: 1. Global distribution based on lightning physics, J. Geophys. Res.-Atmos., 102, 5929–5941, doi:10.1029/96JD03504, 1997. 3604

Querol, X., Alastuey, A., Ruiz, C., Artinano, B., Hansson, H., Harrison, R., Buringh, E. T., Ten Brink, H., Lutz, M., Bruckmann, P., Straehl, P., and Schneider, J.: Speciation and origin of PM_{10} and $PM_{2.5}$ in selected European cities, Atmos. Environ., 38, 6547–6555, 2004. 3595

Remer, L. A., Kleidman, R. G., Levy, R. C., Kaufman, Y. J., Tanré, D., Mattoo, S., Martins, J. V., Ichoku, C., Koren, I., Yu, H., and Holben, B. N.: Global aerosol climatology from the MODIS satellite sensors, J. Geophys. Res.-Atmos., 113, D14S07, doi:10.1029/2007JD009661, 2008. 3604

Rouil, L., Honoré, C., Bessagnet, B., Malherbe, L., Meleux, F., Vautard, R., Beekmann, M., Flaud, J.-M., Dufour, A., Martin, D., Peuch, A., Peuch, V.-H., Elichegaray, C., Poisson, N., and Menut, L.: PREV'AIR: an operational forecasting and mapping system for air quality in Europe, B. Am. Meteorol. Soc., 90, 73–83, 2009. 3597

Ruiz-Arias, J. A., Dudhia, J., Gueymard, C. A., and Pozo-Vázquez, D.: Assessment of the Level-3 MODIS daily aerosol optical depth in the context of surface solar radiation and numerical weather modeling, Atmos. Chem. Phys., 13, 675–692, doi:10.5194/acp-13-675-2013, 2013. 3604

Saiz-Lopez, A. and von Glasow, R.: Reactive halogen chemistry in the troposphere, Chem. Soc. Rev., 41, 6448–6472, doi:10.1039/C2CS35208G, 2012. 3596

Schaap, M., van Loon, M., ten Brink, H. M., Dentener, F. J., and Builtjes, P. J. H.: Secondary inorganic aerosol simulations for Europe with special attention to nitrate, Atmos. Chem. Phys., 4, 857–874, doi:10.5194/acp-4-857-2004, 2004. 3615

Schaap, M., Timmermans, R. M., Roemer, M., Boersen, G., Builtjes, P., Sauter, F., Velders, G., and Beck, J.: The LOTOS-EUROS model: description, validation and latest developments, Int. J. Environ. Pollut., 32, 270–290, 2008. 3600

Seigneur, C., Pun, B., Pai, P., Louis, J.-F., Solomon, P., Emery, C., Morris, R., Zahniser, M., Worsnop, D., Koutrakis, P., White, W., and Tombach, I.: Guidance for the performance evaluation of three-dimensional air quality modeling systems for particulate matter and visibility, JAPCA J. Air Waste Ma., 50, 588–599, doi:10.1080/10473289.2000.10464036, 2000. 3607

Seinfeld, J. and Pandis, S.: Atmospheric Chemistry and Physics, John Wiley, Hoboken, NJ, 1326 pp., 1998. 3602

GMDD
8, 3593–3651, 2015

Sič, B., El Amraoui, L., Marécal, V., Josse, B., Arteta, J., Guth, J., Joly, M., and Hamer, P. D.: Modelling of primary aerosols in the chemical transport model MOCAGE: development and evaluation of aerosol physical parameterizations, Geosci. Model Dev., 8, 381–408, doi:10.5194/gmd-8-381-2015, 2015. 3599, 3600, 3603, 3604, 3609

Slinn, W.: Some approximations for the wet and dry removal of particles and gases from the atmosphere, Water Air Soil Poll., 7, 513–543, 1977. 3603

Slinn, W.: Estimates for the long-range transport of air pollution, in: Long-Range Transport of Airborne Pollutants, Springer, 45–64, 1982. 3603

Stocker, T. F., Qin, D., Plattner, G.-K., Tignor, M., Allen, S. K., Boschung, J., Nauels, A., Xia, Y., Bex, V., and Midgley, P. M.: Climate Change 2013: the Physical Science Basis, Intergovernmental Panel on Climate Change, Working Group I Contribution to the IPCC Fifth Assessment Report (AR5), Cambridge Univ Press, New York, 2013. 3595

Stockwell, W., Kirchner, F., Kuhn, M., and Seefeld, S.: A new mechanism for regional atmospheric chemistry modeling, J. Geophys. Res., 102, 25847–25879, 1997. 3598

Teyssèdre, H., Michou, M., Clark, H. L., Josse, B., Karcher, F., Olivié, D., Peuch, V.-H., Saint-Martin, D., Cariolle, D., Attié, J.-L., Nédélec, P., Ricaud, P., Thouret, V., van der A, R. J., Volz-Thomas, A., and Chéroux, F.: A new tropospheric and stratospheric Chemistry and Transport Model MOCAGE-Climat for multi-year studies: evaluation of the present-day climatology and sensitivity to surface processes, Atmos. Chem. Phys., 7, 5815–5860, doi:10.5194/acp-7-5815-2007, 2007. 3597

Tørseth, K., Aas, W., Breivik, K., Fjæraa, A. M., Fiebig, M., Hjellbrekke, A. G., Lund Myhre, C., Solberg, S., and Yttri, K. E.: Introduction to the European Monitoring and Evaluation Programme (EMEP) and observed atmospheric composition change during 1972–2009, Atmos. Chem. Phys., 12, 5447–5481, doi:10.5194/acp-12-5447-2012, 2012. 3606

Wesely, M.: Parameterization of surface resistances to gaseous dry deposition in regional-scale numerical models, Atmos. Environ., 23, 1293–1304, 1989. 3602

Wexler, A. S. and Seinfeld, J. H.: The distribution of ammonium salts among a size and composition dispersed aerosol, Atmos. Environ. A-Gen., 24, 1231–1246, 1990. 3601

WHO: WHO Air quality guidelines for particulate matter, ozone, nitrogen dioxide and sulfur dioxide: global update 2005: summary of risk assessment, World Health Organization, 2006. 3595

Williamson, D. L. and Rasch, P. J.: Two-dimensional semi-Lagrangian transport with shape-preserving interpolation, Mon. Weather Rev., 117, 102–129, 1989. 3602

GMDD
8, 3593–3651, 2015

Wiscombe, W. J.: Improved Mie scattering algorithms, Appl. Optics, 19, 1505–1509, 1980. 3604
Xu, L. and Penner, J. E.: Global simulations of nitrate and ammonium aerosols and their radiative effects, Atmos. Chem. Phys., 12, 9479–9504, doi:10.5194/acp-12-9479-2012, 2012. 3609
Zhang, J., Reid, J. S., and Holben, B. N.: An analysis of potential cloud artifacts in MODIS over ocean aerosol optical thickness products, Geophys. Res. Lett., 32, L15803, doi:10.1029/2005GL023254, 2005. 3604
Zhuang, H., Chan, C. K., Fang, M., and Wexler, A. S.: Size distributions of particulate sulfate, nitrate, and ammonium at a coastal site in Hong Kong, Atmos. Environ., 33, 843–853, 1999. 3601, 3602, 3631

GMDD
8, 3593–3651, 2015

Table 1. List of the liquid aerosol species given by ISORROPIA model.

Liquid aerosol species
H^+
NA^+
NH_4^+
Cl^-
SO_4^{2-}
HSO_4^-
NO_3^-
H_2O
NH_3
HCl
HNO_3
OH^-

GMDD
8, 3593–3651, 2015

Table 2. List of the solid aerosol species given by ISORROPIA model.

Solid aerosol species
$NaNO_3$
NH_4NO_3
NaCl
Na_2SO_4
$NaHSO_4$
$(NH_4)_2SO_4$
$NAHSO_4$
NH_4HSO_4
$(NH_4)_4H(SO_4)_2$

GMDD
8, 3593–3651, 2015

Table 3. List of the gaseous compounds given by ISORROPIA model.

Gaseous compounds
HCl
HNO_3
NH_3

GMDD
8, 3593–3651, 2015

Table 4. Mass mean aerodynamic diameter of the distribution modes from Zhuang et al. (1999).

mode in µm	Sulfates	Ammoniums	Nitrates
Condensation mode	0.2 ± 0.15	0.21 ± 0.10	0.14 ± 0.22
Droplet mode	0.58 ± 0.11	0.56 ± 0.10	0.46 ± 0.33
Coarse mode	4.2 ± 2	5.7 ± 2	3.95 ± 0.69

GMDD
8, 3593–3651, 2015

Table 5. Secondary inorganic aerosol compound statistics of RACMSIA simulation daily HTAP observations.

Compound	number of stations	number of observations	MNMB	FGE	Correlation
Sulfate total	94	30 754	−0.32	0.79	0.52
Sulfate corrected	21	7098	−0.12	0.73	0.70
Nitrate	61	19 410	−0.13	0.94	0.53
Ammonium	51	15 765	0.19	0.74	0.69

GMDD
8, 3593–3651, 2015

Table 6. Statistics of daily observation at the same Irish as in Fig. 7 against RACMSIA simulation.

Compound	MNMB	FGE	Correlation
Sulfate	−0.19	0.53	0.65
Nitrate	0.17	0.54	0.77
Ammonium	0.02	0.46	0.71

GMDD
8, 3593–3651, 2015

Table 7. Gaseous compounds statistics of simulation results against daily HTAP observations. Comparison between a simulation with SIA (RACMSIA) and without SIA formation (RACM).

			MNMB		FGE		Correlation	
Compound	number of stations	number of observations	RACM	RACMSIA	RACM	RACMSIA	RACM	RACMSIA
Sulfur dioxide	69	23 325	1.21	1.21	1.37	1.37	0.53	0.53
Nitrogen dioxide	41	14 122	0.61	0.53	0.83	0.77	0.55	0.57
Nitric acid	30	10 033	0.45	−0.13	0.88	0.99	0.46	0.33
Ammonia	20	6381	1.84	0.79	1.84	1.27	0.18	0.33

GMDD
8, 3593–3651, 2015

Table 8. Secondary inorganic aerosol compounds statistics of RACMSIA simulation against weekly HTAP observations.

Compound	number of stations	number of observations	MNMB	FGE	Correlation
Sulfate total	192	19 203	−0.1	0.68	0.66
Sulfate corrected	1	52	−0.12	0.63	0.51
Nitrate	190	19 066	0.06	1.00	0.41
Ammonium	43	1595	0.34	0.84	0.43

GMDD
8, 3593–3651, 2015

Table 9. Secondary inorganic aerosol compounds statistics of RACMSIA simulation against weekly HTAP observations, separation between North America (N. A.) and Asia.

	Stations		MNMB		FGE		Correlation	
Compound	N. A.	Asia	N. A.	Asia	N. A.	Asia	N. A.	Asia
Sulfate total	161	28	−0.09	−0.17	0.66	0.95	0.67	0.38
Nitrate	161	28	0.05	0.30	0.99	1.16	0.41	0.13
Ammonium	14	28	0.27	0.35	0.60	0.96	0.19	0.41

GMDD
8, 3593–3651, 2015

Table 10. Secondary inorganic aerosols statistics of RACMSIA simulation against daily EMEP observations.

Compound	number of stations	number of observations	MNMB	FGE	Correlation
Sulfate total	66	19 861	−0.36	0.75	0.58
Sulfate corrected	34	9705	−0.33	0.73	0.68
Nitrate	49	13 360	−0.08	0.87	0.53
Ammonium	40	10 406	0.18	0.69	0.71

GMDD
8, 3593–3651, 2015

Table 11. Gaseous compounds statistics of simulation results against daily EMEP observations. Comparison between a simulation with SIA (RACMSIA) and without SIA formation (RACM).

			MNMB		FGE		Correlation	
Compound	number of stations	number of observations	RACM	RACMSIA	RACM	RACMSIA	RACM	RACMSIA
Sulfur dioxide	47	14 861	0.97	0.98	1.15	1.15	0.60	0.60
Nitrogen dioxide	44	14 809	0.18	0.10	0.74	0.69	0.57	0.59
Nitric acid	12	3290	0.55	−0.15	0.99	1.08	0.36	0.26
Ammonia	40	5324	1.61	0.46	1.62	1.18	−0.01	0.24

GMDD
8, 3593–3651, 2015

Table 12. Air quality regulated pollutants statistics of simulations against hourly AIRBASE observations. Comparison between a simulation with SIA (RACMSIA) and without SIA formation (RACM).

		MNMB		FGE		Correlation	
Compound	number of Stations	RACM	RACMSIA	RACM	RACMSIA	RACM	RACMSIA
$PM_{2.5}$	1082	−0.58	−0.14	0.77	0.56	0.58	0.47
PM_{10}	1082	−0.89	−0.45	0.97	0.66	0.39	0.50
O_3	1168	0.31	0.27	0.42	0.41	0.63	0.60
NO_2	610	−0.10	−0.13	0.66	0.65	0.54	0.53

GMDD
8, 3593–3651, 2015

Table 13. Comparison of MNMB statistics between MOCAGE simulations (RACM and RACM-SIA) and AIRBASE data over Europe for $PM_{2.5}$ according to different seasons.

$PM_{2.5}$ MNMB	RACM	RACMSIA	Δ
Year	−0.58	−0.14	+0.44
MAM	−0.55	−0.03	+0.52
JJA	−0.62	−0.27	+0.35
SON	−0.44	−0.07	+0.37

GMDD
8, 3593–3651, 2015

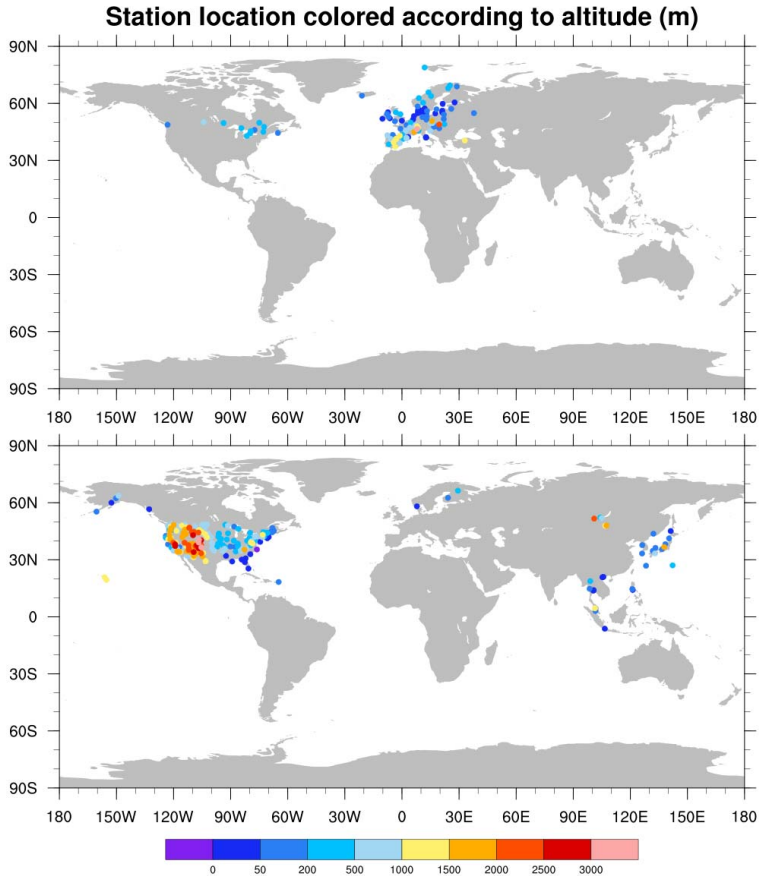

Figure 1. Maps with the location of the stations measuring in 2005 total sulfate from the HTAP database used to evaluate the model. Colors represent the altitude of the stations. The upper panel represents daily observation stations while the bottom panel represents weekly observation stations.

GMDD
8, 3593–3651, 2015

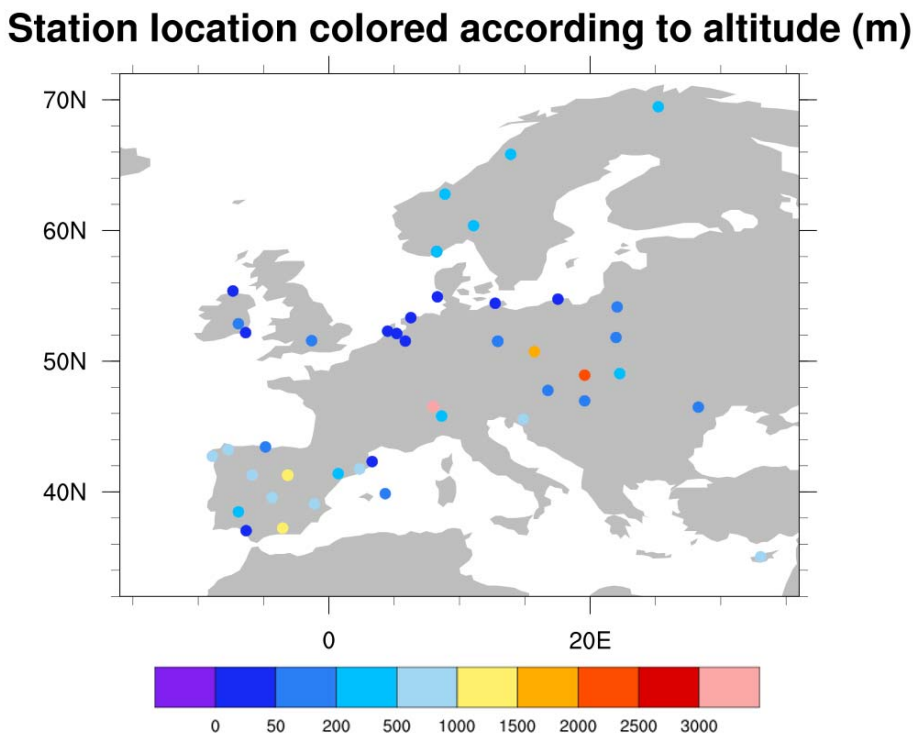

Figure 2. Map with the location of the stations measuring in 2010 daily nitrate from the EMEP database used to evaluate the regional model results. The domain plotted corresponds to the limit of the regional domain of the simulation. Colors represent the altitude of the stations.

GMDD
8, 3593–3651, 2015

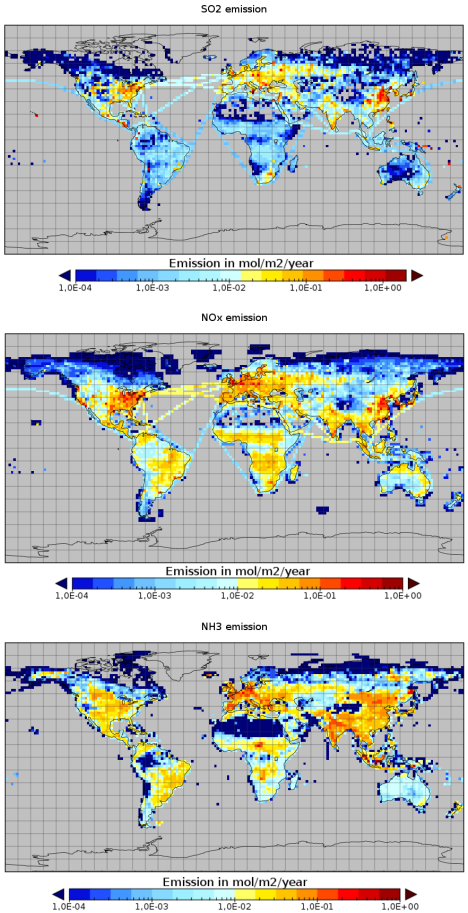

Figure 3. Maps of 2005 annual emissions of sulfur dioxide (SO_2) (top panel), nitrous oxides (NO_x) (middle panel) and ammonia (NH_3) (bottom panel), in mol m^{-2} $year^{-1}$ for the MOCAGE simulations (RACM and RACMSIA).

GMDD
8, 3593–3651, 2015

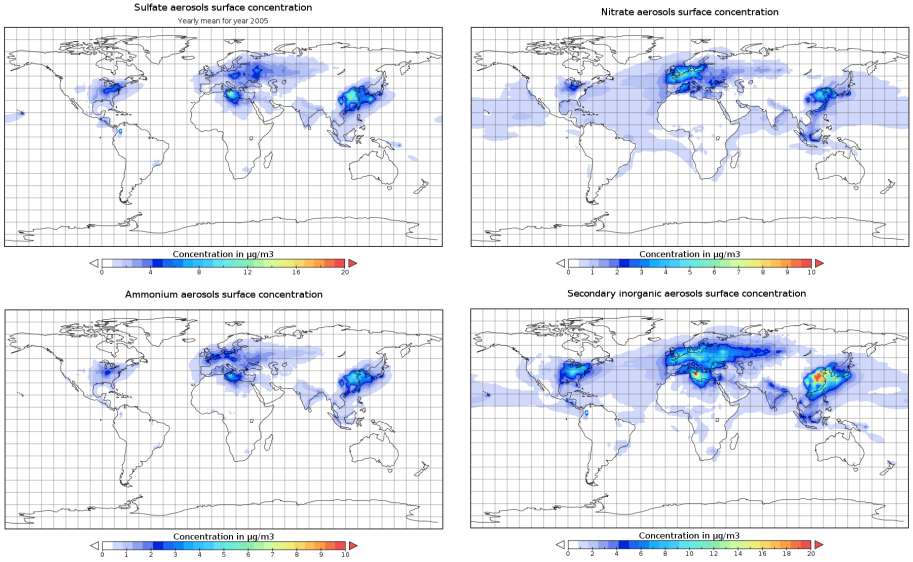

Figure 4. Maps of global annual mean concentrations at the surface, in $\mu g\,m^{-3}$ of secondary inorganic aerosols components from the RACMSIA simulation. Top left panel is sulfate, top right panel nitrate, bottom left panel ammonium and bottom right panel is the sum of the three components.

GMDD
8, 3593–3651, 2015

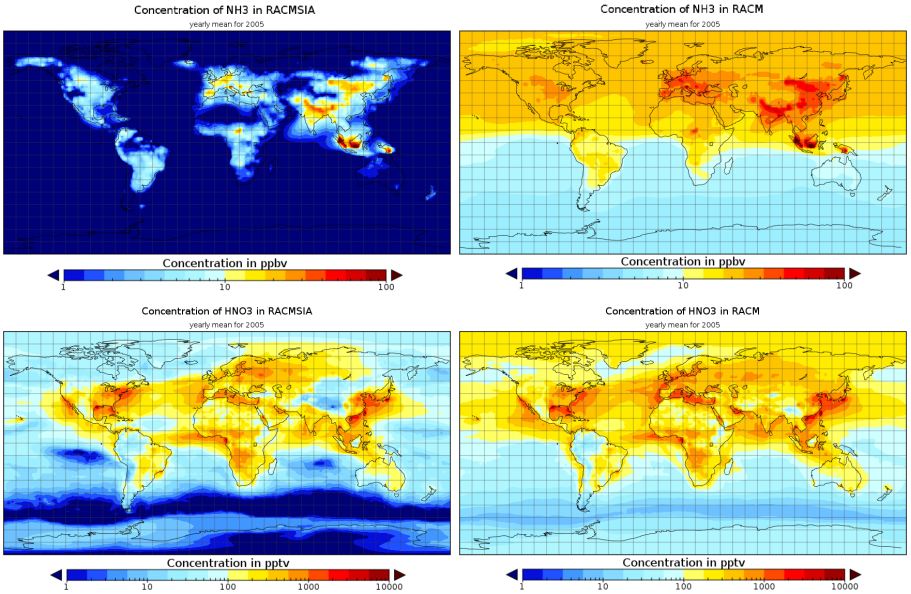

Figure 5. Maps of global annual mean concentrations of NH_3 in ppbv (top panels) and HNO_3 in pptv (bottom panels) for both simulations RACMSIA (left side) and RACM (right side).

GMDD
8, 3593–3651, 2015

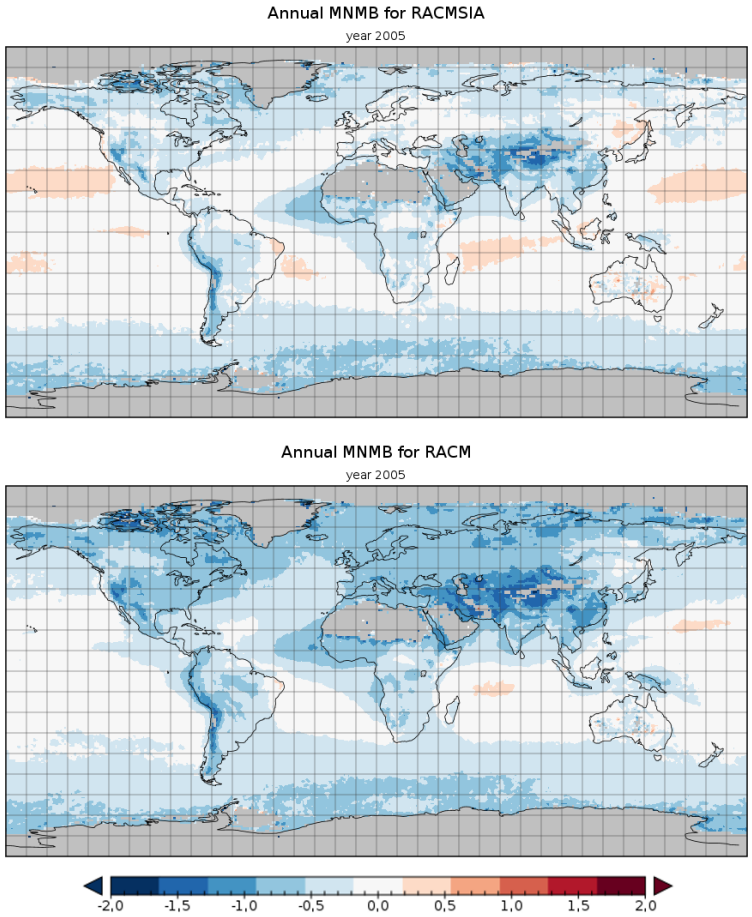

Figure 6. Maps of annual modified normalised mean bias (MNMB) of aerosol optical depth against MODIS observations. The upper panel shows the RACM experiment while the lower panel the RACMSIA experiment with secondary inorganic aerosols.

GMDD
8, 3593–3651, 2015

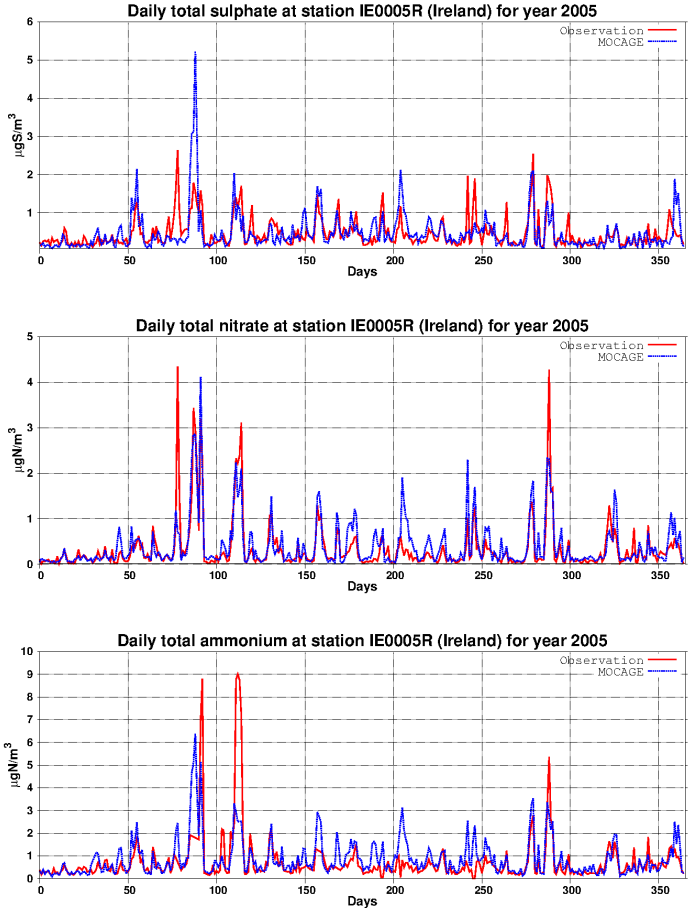

Figure 7. Time-series of daily values (in $\mu g\,m^{-3}$) of sulfate (top panel), nitrate (middle panel) and ammonium (bottom panel) at an Irish station (52.87° N; 6.92° W) against RACMSIA simulation for the year 2005.

GMDD
8, 3593–3651, 2015

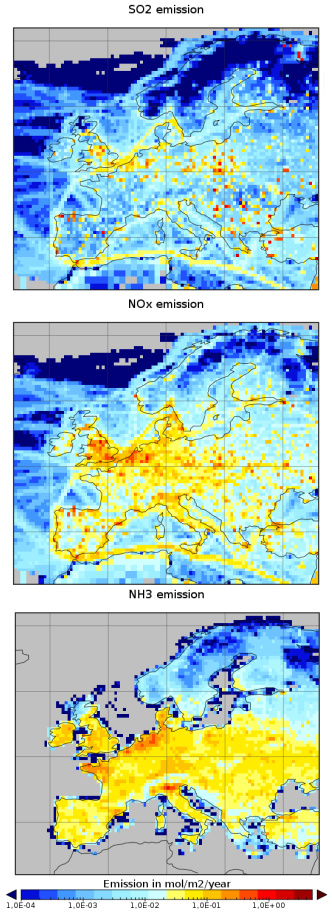

Figure 8. Maps of annual emissions for sulfur dioxide (top panel), nitrous oxides (middle panel) and ammonia (bottom panel) in mol m^{-2} $year^{-1}$ for the MOCAGE simulations (RACM and RACMSIA).

GMDD
8, 3593–3651, 2015

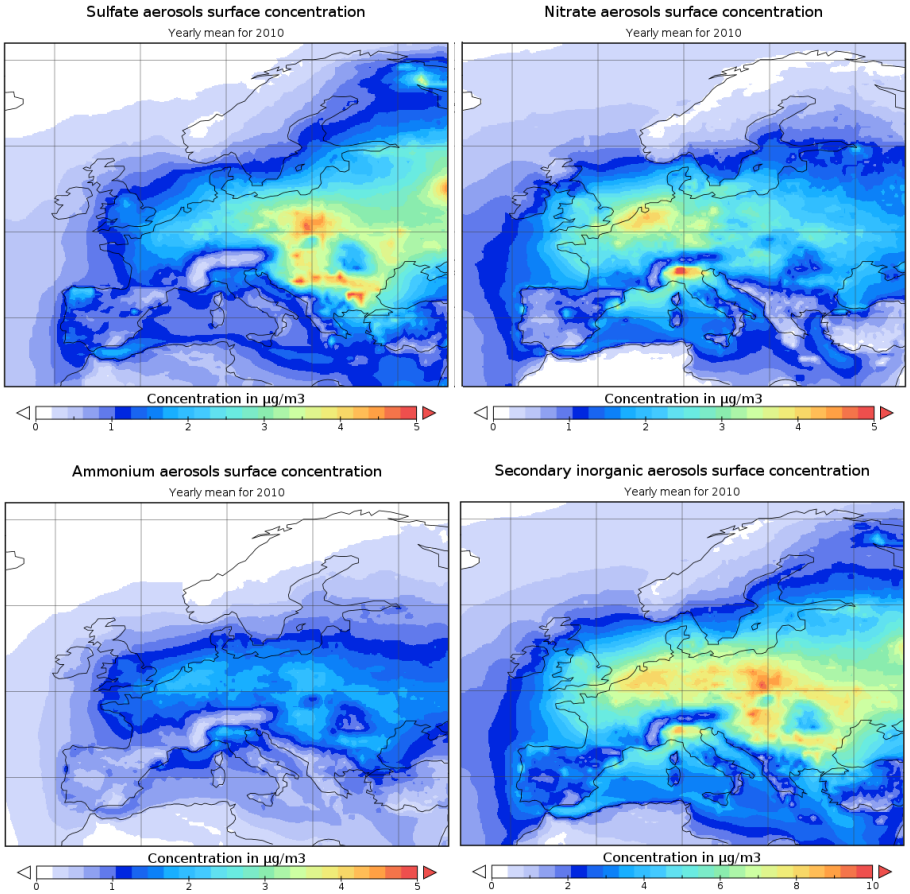

Figure 9. Maps of regional annual mean concentrations, in $\mu g\,m^{-3}$ of secondary inorganic aerosols components over a regional domain for the year 2010 for the RACMSIA simulation. Top left panel represents sulfate concentration, top right nitrate, bottom left ammonium and bottom right represents the sum of these three SIA components.

GMDD
8, 3593–3651, 2015

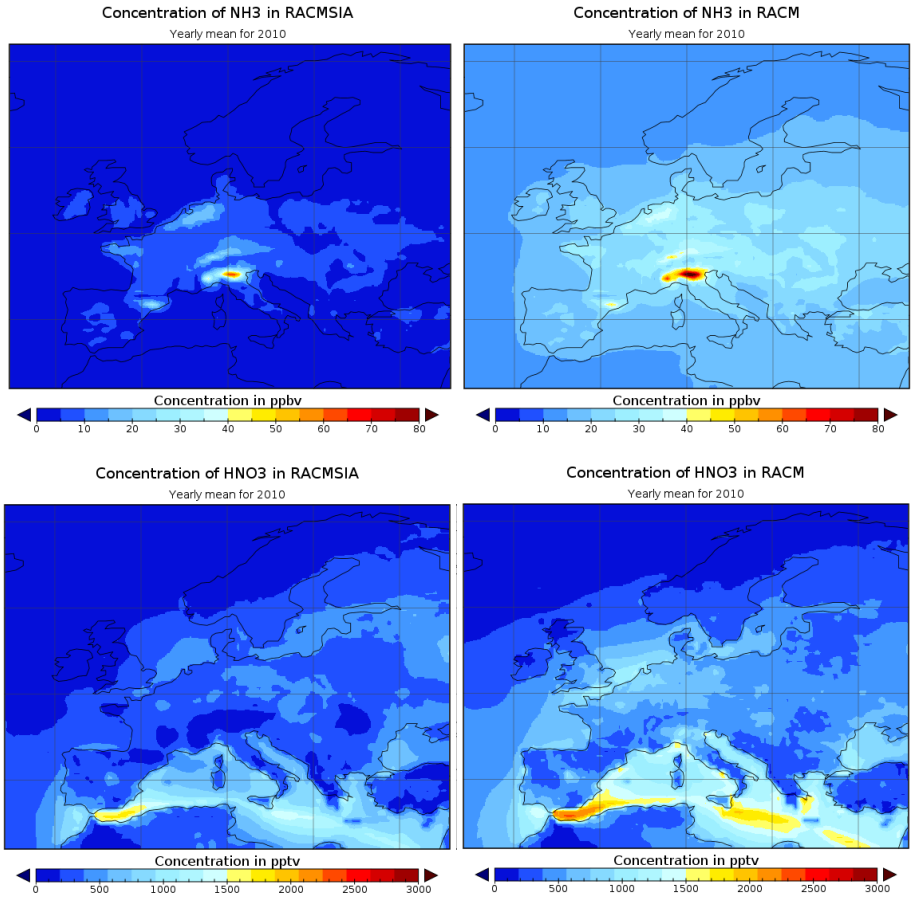

Figure 10. Maps of regional annual mean concentrations of NH_3 in ppbv (top panels) and HNO_3 in pptv (bottom panels) for both simulations RACMSIA (left side) and RACM (right side).

GMDD
8, 3593–3651, 2015

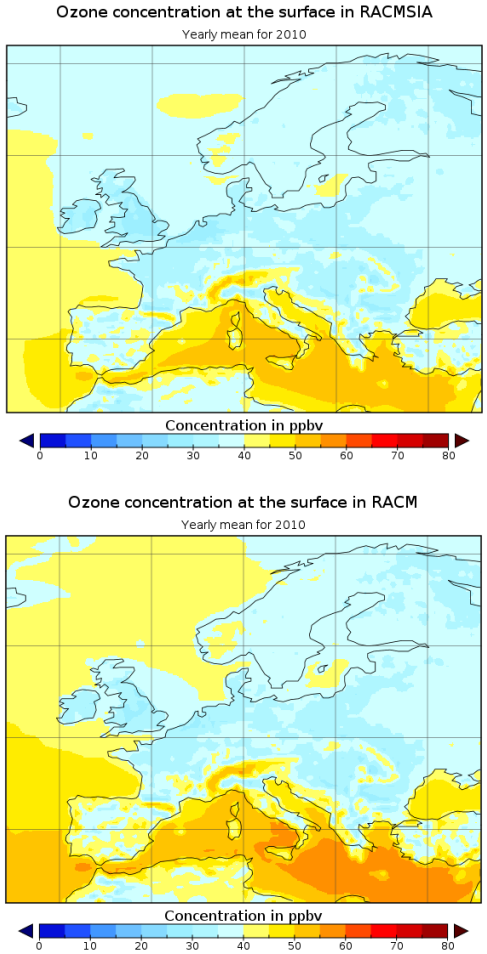

Figure 11. Maps of regional annual mean ozone concentrations for the year 2010 in ppbv. Top panel represents RACMSIA simulation and bottom panel the RACM simulation.

GMDD
8, 3593–3651, 2015